ANALYTICAL SOLUTION FOR NONLINEAR BENDING OF FG PLATES BY A LAYERWISE THEORY

M. Tahani*, S.M. Mirzababaee**
***Department of Mechanical Engineering, Ferdowsi University of Mashhad, Mashhad, Iran**
****Khorasan Research Center for Technology Development (KRCTD), Quchan Highway, Mashhad, Iran**

Keywords: *Functionally graded materials, Geometric nonlinearity, Plates, Analytical solution, Layerwise method*

Abstract

A layerwise theory is used to analyze analytically displacements and stresses in functionally graded (FG) composite plates in cylindrical bending subjected to thermomechanical loadings. The plates are assumed to have isotropic, two-constituent material distribution through the thickness, and the modulus of elasticity of the plate is assumed to vary according to a power-law distribution in terms of the volume fractions of the constituents. The nonlinear strain-displacement relations in the von Kármán sense are used to study the effect of geometric nonlinearity. The equilibrium equations are solved exactly and also by using a perturbation technique. Numerical results are presented to show the effect of the material distribution on the deflections and stresses.

1 Introduction

In conventional laminated composite materials, there is a high chance that debonding will occur at some extreme loading conditions. On the other hand, gradually varying the volume fraction of the constituents can resolve this problem. Functionally graded materials (FGMs) are composite materials which exhibit a progressive change in composition, structure, and properties as a function of spatial direction within the material.

Many studies for thermal stress and linear thermal bending of FGM plates are available in the literature (e.g, see [1-3]). However, investigations in nonlinear analysis of FGM plates under thermal or mechanical loading are limited in number. For example, Praveen and Reddy [4] investigated the response of functionally graded ceramic-metal plates using a plate finite element that accounts for the transverse shear strains, rotary inertia and moderately large rotations in the von Kármán sense. Reddy [5] presented solutions for rectangular functionally graded plates based on the third-order shear deformation plate theory. The formulation accounted for the thermomechanical coupling, time dependency, and the von Kármán-type geometric nonlinearity. Using an asymptotic method, the three-dimensional thermo-mechanical deformations of functionally graded rectangular plate were investigated by Reddy and Cheng [6] and the distributions of temperature, displacements and stresses in the plate were calculated for different volume fraction of ceramic constituent.

Shen [7] analyzed nonlinear bending of a simply supported, functionally graded rectangular plate subjected to a transverse uniform or sinusoidal load and in thermal environments. He obtained governing equations based on Reddy's higher-order shear deformation plate theory and solved them by a mixed Galerkin-perturbation technique. Based on the von Kármán theory, Woo and Meguid [8] derived an analytical solution expressed in terms of Fourier series for the large deflection of functionally graded plates and shallow shells under transverse mechanical loading and a temperature field. Yang and Shen [9] using a semi-analytical approach analyzed the nonlinear bending and post-buckling behaviors of FG rectangular plates subjected to combined action of transverse and in-plane loads. Tahani et al. [10] analytically analyzed functionally graded beams subjected to thermomechanical loadings based on a first-order shear deformation theory. Hsieh and Lee [11] solved the inverse problem of a functionally

graded elliptical plate with large deflection and disturbed boundary under uniform load. They derived the governing equations of a thin plate with large deflection based on the classical nonlinear von Kármán plate theory. Then they employed a perturbation technique on displacement terms in conjunction with Taylor series expansion of the disturbed boundary conditions to solve the non-classical problem. Agarwal et al. [12] used the existing statically exact beam finite element based on the first order shear deformation theory to study the geometric nonlinear effects on static and dynamic responses in isotropic, composite and functionally graded material beams. They utilized both von Kármán strain tensor and Green's strain tensor in the static case, whereas, for the wave propagation studies only the von Kármán strains were used.

It is intended here to accurately determine the displacements and stresses in functionally graded plates in cylindrical bending subjected to thermomechanical loadings. To this end, based on a layerwise theory the governing equations are obtained. Also, the nonlinear strain-displacement relations are used to study the effect of geometric nonlinearity. The equilibrium equations are solved exactly for FGM plates with the same boundary conditions and also by using a perturbation technique for FGM plates with general boundary conditions. Numerical results are presented to show the influence of material properties, plate geometry, mechanical loading and the temperature field on the resulting transverse deflection and stress state.

2 Theoretical Formulation

2.1 Displacement Field and Strains

Consider a functionally graded plate of thickness h, length a in the x-direction, and infinite extent in the y-direction. Since the plate is long, it may safely be assumed that a state of plane strain exists. Hence, the following displacement field is assumed:

$$\begin{aligned} &u_1(x,y,z) = u_0(x) + U_k(x)\Phi_k(z) \\ &u_2(x,y,z) = 0 \qquad\qquad k = 1,2,\ldots,N+1 \\ &u_3(x,y,z) = w(x) \end{aligned} \tag{1}$$

It is to be noted that a repeated index indicates summation over all values of that index. In Eqs. (1) u_0 and w are the displacement of the points in the middle surface of the plate in the x- and z-directions, respectively, U_k (k=1,2,…, N+1) is the displacement component of all points located on the kth plane in the x-direction, and Φ_k is a continuous function of the thickness coordinate z (global interpolation function). Also N denotes the total number of numerical layers considered in a plate.

In the present study we wish to investigate the effect of geometric non-linearity on the response quantities. Therefore, the von Kármán-type of geometric non-linearity is taken into consideration in the strain-displacement relations. Substituting Eqs. (1) in the appropriate strain-displacement relations [13] results in:

$$\begin{aligned} &\varepsilon_x = u_0' + (w')^2/2 + U_k'\Phi_k \\ &\varepsilon_y = \varepsilon_z = \gamma_{xy} = \gamma_{yz} = 0 \\ &\gamma_{xz} = w' + U_k\Phi_k' \end{aligned} \tag{2}$$

where a prime indicates an ordinary derivative with respect to the corresponding independent variable.

2.2 Constitutive Relations

We consider a functionally graded plate, which is made from a mixture of ceramics and metals. It is assumed that the composition properties of FGM vary through the thickness of the plate. The variation of material properties can be expressed as:

$$p(z) = (p_t - p_b)V_t + p_b \tag{3}$$

where p denotes a generic material property like modulus, p_t and p_b denote the corresponding properties of the top and bottom faces of the plate, respectively. Also V_t in Eq. (3) denotes the volume fraction of the top face constituent and follows a simple power-law as:

$$V_t = \left(\frac{z}{h} + \frac{1}{2}\right)^n \tag{4}$$

where z is the thickness coordinate ($-h/2 \le z \le h/2$) and n is a parameter that dictates the material variation profile through the thickness.

Here we assume that moduli E and G, coefficient of thermal expansion α, and thermal conductivity k vary according to Eq. (3) and the Poisson's ratio ν is assumed to be a constant.

The linear constitutive relations are:

$$\begin{Bmatrix} \sigma_x \\ \sigma_y \\ \sigma_{xy} \end{Bmatrix} = \begin{bmatrix} Q_{11} & Q_{12} & 0 \\ Q_{12} & Q_{22} & 0 \\ 0 & 0 & Q_{66} \end{bmatrix} \left(\begin{Bmatrix} \varepsilon_x \\ \varepsilon_y \\ \gamma_{xy} \end{Bmatrix} - \begin{pmatrix} 1 \\ 1 \\ 0 \end{pmatrix} \alpha \Delta T \right)$$

$$\begin{Bmatrix}\sigma_{yz}\\ \sigma_{xz}\end{Bmatrix}=\begin{bmatrix}Q_{44} & 0\\ 0 & Q_{55}\end{bmatrix}\begin{Bmatrix}\gamma_{yz}\\ \gamma_{xz}\end{Bmatrix} \tag{5}$$

where

$$\begin{aligned} Q_{11}=Q_{22}&=\frac{E(z)}{1-\nu^2}, \quad Q_{12}=\frac{\nu E(z)}{1-\nu^2}\\ Q_{44}=Q_{55}=Q_{66}&=\frac{E(z)}{2(1+\nu)}=G(z)\end{aligned} \tag{6}$$

and ΔT is the temperature change from a stress-free state that will be obtained by solving the one-dimensional heat transfer equation.

2.3 Equilibrium Equations

Using the principle of minimum total potential energy [13], the equilibrium equations can be shown to be:

$$\delta u_0: \quad \frac{dN_x}{dx}=0 \tag{7a}$$

$$\delta U_k: \quad \frac{dM_x^k}{dx}-Q_x^k=0 \tag{7b}$$

$$\delta w: \quad \frac{dQ_x}{dx}+\frac{d}{dx}\left(N_x\frac{dw}{dx}\right)+q(x)=0 \tag{7c}$$

where $q(x)$ is the transverse load on the top surface of the plate. In Eqs. (7) the generalized stress resultants are defined as:

$$\begin{aligned}(N_x,Q_x)&=\int_{-h/2}^{h/2}(\sigma_x,\sigma_{xz})dz\\ (M_x^k,Q_x^k)&=\int_{-h/2}^{h/2}(\sigma_x\Phi_k,\sigma_{xz}\Phi_k')dz\end{aligned} \tag{8}$$

The boundary conditions consist of specifying the following quantities at $x=\pm a/2$:

Geometric (Essential)	Force (Natural)
u_0	N_x
U_k	M_x^k
w	$N_x w'+Q_x$

(9)

Upon substitution of Eqs. (5) into Eqs. (8), the generalized stress resultants in terms of displacement components will be obtained which can be presented as follows:

$$\begin{aligned} N_x&=A_{11}[u_0'+(w')^2/2]+B_{11}^jU_j'-N_x^T\\ M_x^k&=B_{11}^k[u_0'+(w')^2/2]+D_{11}^{kj}U_j'-M_x^{k(T)}\\ Q_x&=A_{55}w'+A_{55}^jU_j\\ Q_x^k&=A_{55}^kw'+A_{55}^{kj}U_j\end{aligned} \tag{10}$$

where

$$\begin{aligned} A_{ij}&=\sum_{i=1}^N\int_{z_i}^{z_{i+1}}Q_{ij}^{(i)}dz, \quad ij=11,55\\ A_{55}^k&=\sum_{i=1}^N\int_{z_i}^{z_{i+1}}Q_{55}^{(i)}\Phi_k'dz\\ B_{11}^k&=\sum_{i=1}^N\int_{z_i}^{z_{i+1}}Q_{11}^{(i)}\Phi_kdz\\ A_{55}^{kj}&=\sum_{i=1}^N\int_{z_i}^{z_{i+1}}Q_{55}^{(i)}\Phi_k'\Phi_j'dz\\ D_{11}^{kj}&=\sum_{i=1}^N\int_{z_i}^{z_{i+1}}Q_{11}^{(i)}\Phi_k\Phi_jdz\end{aligned} \tag{11}$$

The thermal resultants in Eqs. (10) are defined as:

$$(N_x^T,M_x^{k(T)})=\sum_{i=1}^N\int_{z_i}^{z_{i+1}}Q_{11}^{(i)}(1,\Phi_k)\alpha\Delta Tdz \tag{12}$$

Lastly, the governing equations of equilibrium are obtained by substituting Eqs. (10) into Eqs. (7).

3 Analytical Solutions

In this section a functionally graded plate subjected to a uniform transverse load on its top surface and/or thermal load is considered. In order to solve the equilibrium equations in thermal loadings the temperature field should be known. It is assumed that one value of temperature is imposed on the bottom surface and the other value on the top surface of the plate. In this case, the temperature distribution through the thickness can be obtained by solving a simple steady state heat transfer equation through the thickness of the plate. This equation is given by:

$$-\frac{d}{dz}\left(k(z)\frac{dT}{dz}\right)=0 \tag{13}$$

and the boundary conditions are $T=T_b$ at $z=-h/2$ and $T=T_t$ at $z=h/2$. It is readily seen that the solution to Eq. (13) is:

$$T(\xi)=c_{1n}hA_n(\xi)/(k_t-k_b)+c_{2n} \tag{14}$$

where

$$\xi=\frac{z}{h}+\frac{1}{2}, \quad A_n(\xi)=\int\frac{d\xi}{\xi^n-\mu^n}$$

$$c_{1n}=\frac{(T_t-T_b)(k_t-k_b)}{h[A_n(1)-A_n(0)]}$$

$$c_{2n} = \frac{T_t A_n(0) - T_b A_n(1)}{A_n(1) - A_n(0)} \tag{15}$$

with $\mu^n = k_b/(k_b - k_t)$. It is to be noted that the integral of $A_n(\xi)$ in Eqs. (15) has analytical solution for n=0.2, n=0.5, and all integer values. For other values of n, this integral must be solved numerically.

In what follows two solution methodologies for Eqs. (7) are presented.

3.1 Exact Solutions

In this section, the boundary conditions of the plate at $x = \pm a/2$ are assumed to be the same. Before discussing the procedure adopted for solving Eqs. (7), it is appropriate to indicate here that in this layerwise theory two types of simple supports at the edges of the plate (i.e., at $x = \pm a/2$) may be classified, namely:

$$\text{S1:} \quad u_0 = M_x^k = W_k = 0 \tag{16a}$$

$$\text{S3:} \quad N_x = M_x^k = W_k = 0 \tag{16b}$$

also two types of clamped supports may be classified, namely:

$$\text{C1:} \quad u_0 = U_k = W_k = 0 \tag{17a}$$

$$\text{C3:} \quad N_x = U_k = W_k = 0 \tag{17b}$$

It is to be noted that these types of boundary conditions are defined similar to the definitions in the equivalent single-layer theories. For simplicity, the boundary conditions of a composite plate in cylindrical bending may be represented in a concise rule. For example, a plate with the edge conditions C1 at $x = -a/2$ and S3 at $x = a/2$ may be called C1-S3.

In order to obtain the exact solutions of equilibrium Eqs. (7), Eq. (7a) is integrated with respect to x to yield:

$$\begin{aligned} &N_x = N_x^0 \quad \text{or} \\ &A_{11}[u_0' + (w')^2/2] + B_{11}^j U_j' = N_x^0 + N_x^T \end{aligned} \tag{18}$$

where N_x^0 is a constant of integration. Next we solve Eq. (18) to obtain:

$$u_0' + (w')^2/2 = (N_x^0 + N_x^T - B_{11}^j U_j')/A_{11} \tag{19}$$

Subtituting Eq. (19) into Eq. (10) and the subsequent results into Eqs. (7b) and (7c) to yield:

$$\left(D_{11}^{kj} - \frac{B_{11}^k B_{11}^j}{A_{11}}\right) U_j'' - A_{55}^{kj} U_j - A_{55}^k w' = 0 \tag{20a}$$

$$A_{55}^j U_j' + (A_{55} + N_x^0) w'' = -q(x) \tag{20b}$$

Eqs. (20) are N+2 linear ordinary differential equations with constant coefficients. It is to be noted that there exist repeated zero roots (or eigenvalues) in the characteristic equation of the set of equations in (20). In order to enhance the solution scheme of these equations, some small artificial terms will be added to these equations so that the characteristic roots become all distinct (see [14]):

$$\left(D_{11}^{kj} - \frac{B_{11}^k B_{11}^j}{A_{11}}\right) U_j'' - A_{55}^{kj} U_j - A_{55}^k w' = \varepsilon^{kj} U_j \tag{21a}$$

$$A_{55}^j U_j' + (A_{55} + N_x^0) w'' = -q(x) + \varepsilon w \tag{21b}$$

where

$$\varepsilon^{kj} = \varepsilon \int_{-h/2}^{h/2} \Phi_k \Phi_j \, dz \tag{22}$$

with ε being a prescribed small number.

Next, Eqs. (21) can be solved analytically for any sets of boundary conditions in terms of the unknown constant N_x^0. After solving these equations, we will use one more condition to find the final solutions. In order to solve Eqs. (21), for convenience, the following state space variables are introduced:

$$\begin{aligned} &\{X_1(x)\} = \{U(x)\}, \quad \{X_2(x)\} = \{U'\} = \{X_1'\} \\ &X_3(x) = w(x), \quad X_4(x) = w' = X_3' \end{aligned} \tag{23}$$

where $\{X_1\}^T = [U_1, U_2, ..., U_{N+1}]$.

Substitution of Eqs. (23) into Eqs. (21) results in a system of 2N+4 coupled first-order ordinary differential equations which, on the other hand, may be presented as:

$$\{X'\} = [A]\{X\} + \{F\} \tag{24}$$

with $\{X\}^T = [\{X_1\}^T, \{X_2\}^T, X_3, X_4]$. In Eq. (24) the coefficient matrix $[A]$ and vector $\{F\}$ are presented in Appendix. The general solutions of Eq. (24) are given by (e.g. see [15]):

$$\begin{aligned} \{X\} &= [\mathbf{U}][Q(\lambda x)]\{K\} \\ &+ [\mathbf{U}][Q(\lambda x)] \int [Q(\lambda x)]^{-1} [\mathbf{U}]^{-1} \{F\} dx \end{aligned} \tag{25}$$

with $[Q(\lambda x)] = \text{diag}(e^{\lambda_1 x}, e^{\lambda_2 x}, ..., e^{\lambda_{2N+4} x})$ and $\{K\}$ being 2N+4 arbitrary unknown constants of integration to be found by imposing the boundary conditions. Here, $[\mathbf{U}]$ and λ_k $(k = 1, 2, ..., 2N+4)$ are, respectively, the matrix of eigenvectors and

eigenvalues of the coefficient matrix [A] which, in general, must be regarded to have complex values.

Next, in order to obtain N_x^0 we note that, for example, for the C1-C1 and S1-S1 boundary types we have u_0=0 at $x=\pm a/2$ which will allow us to find N_x^0 in a trial and error process. Towards this end, we note that integrating Eq. (19) from 0 to a/2 results in:

$$[u_0]\Big|_{x=0}^{x=a/2} = \int_0^{a/2}\left[\frac{N_x^0 + N_x^T - B_{11}^j U_j'}{A_{11}} - \frac{1}{2}(w')^2\right]dx \qquad (26)$$

Clearly, because of symmetry we have $u_0(0)$=0. Therefore, we conclude that:

$$N_x^0 = \frac{2A_{11}}{a}\int_0^{a/2}\left[\frac{B_{11}^j U_j'}{A_{11}} + \frac{1}{2}(w')^2\right]dx - N_x^T \qquad (27)$$

By making the solutions of the Eqs. (25) to satisfy (27) in a trial and error process, we will obtain the exact value of N_x^0. Finally, u_0 will be obtained by integrating Eq. (19) as:

$$u_0 = -\int \frac{1}{2}(w')^2\,dx + \frac{N_x^0 + N_x^T}{A_{11}}x - \frac{B_{11}^j U_j}{A_{11}} \qquad (28)$$

3.2 Perturbation technique

In this section, Lindstedt-Poincaré method is used to solve the three coupled nonlinear ordinary differential equations appearing in (7). To this end, we define W_0 as follows:

$$w(0) = W_0 \qquad (29)$$

Also the unknown variables in Eqs. (7) are represented by the following expansions:

$$u_0(x) = u_1(x)W_0^1 + u_2(x)W_0^2 + u_3(x)W_0^3 + \cdots \qquad (30a)$$

$$U_k(x) = U_k^1(x)W_0^1 + U_k^2(x)W_0^2 + U_k^3(x)W_0^3 + \cdots \qquad (30b)$$

$$w(x) = w_1(x)W_0^1 + w_2(x)W_0^2 + w_3(x)W_0^3 + \cdots \qquad (30c)$$

where W_0 is an unknown parameter which will be found at the end of analysis. Next, in mechanical loading ($\Delta T = 0$) we let:

$$q = q_1 W_0^1 + q_2 W_0^2 + q_3 W_0^3 + \cdots \qquad (31)$$

Also in thermal loading ($q(x) = 0$) we consider the change of temperature of the top surface of the plate as ΔT. Using Eq. (13) we can derive the temperature field in terms of ΔT. Finally, in this case, we let:

$$\Delta T = \Delta T_1 W_0^1 + \Delta T_2 W_0^2 + \Delta T_3 W_0^3 + \cdots \qquad (32)$$

where q_i's and ΔT_i's are some unknown constants which will be found by imposing certain conditions. These conditions are found by noting that from (29) and (30c) we must conclude that:

$$\begin{aligned} &w_1(0) = 1 \\ &w_i(0) = 0, \quad i = 2, 3, \ldots \end{aligned} \qquad (33)$$

Substituting Eqs. (30) and (31) into Eqs. (7), results in infinite sets of coupled ordinary linear differential equations. For example, three first sets of equations for mechanical loading case are:

W_0^1:

$$\begin{aligned} &A_{11}u_1'' + B_{11}^j U_j^{1\prime} = 0 \\ &B_{11}^k u_1'' + D_{11}^{kj} U_j^{1\prime\prime} - A_{55}^{kj} U_j^1 - A_{55}^k w_1' = 0 \\ &A_{55} w_1'' + A_{55}^j U_j^{1\prime} = -q_1 \end{aligned} \qquad (34)$$

W_0^2:

$$\begin{aligned} &A_{11}u_2'' + B_{11}^j U_j^{2\prime} = -A_{11} w_1' w_1'' \\ &B_{11}^k u_2'' + D_{11}^{kj} U_j^{2\prime\prime} - A_{55}^{kj} U_j^2 - A_{55}^k w_2' = -B_{11}^k w_1' w_1'' \\ &A_{55} w_2'' + A_{55}^j U_j^{2\prime} = -q_2 - A_{11} u_1' w_1'' - B_{11}^j U_j^{1\prime} w_1'' \end{aligned} \qquad (35)$$

W_0^3:

$$\begin{aligned} &A_{11}u_3'' + B_{11}^j U_j^{3\prime} = -A_{11}(w_1' w_2'' + w_2' w_1'') \\ &B_{11}^k u_3'' + D_{11}^{kj} U_j^{3\prime\prime} - A_{55}^{kj} U_j^3 - A_{55}^k w_3' = \\ &\qquad - B_{11}^k (w_1' w_2'' + w_2' w_1'') \\ &A_{55} w_3'' + A_{55}^j U_j^{3\prime} = -q_3 \\ &\qquad - A_{11}[u_1' w_2'' + u_2' w_1'' + (w_1')^2/2] \\ &\qquad - B_{11}^j (U_j^{1\prime} w_2'' + U_j^{2\prime} w_1'') \end{aligned} \qquad (36)$$

After the solution for these sets of equations are obtained, then constants q_i's (or ΔT_i's) are found by imposing the conditions in (33). Finally W_0 is found by numerically solving the polynomial equation in (31) (or (32)).

4 Numerical results and discussion

The solution procedures outlined in the previous section are applied to functionally graded plates subjected to a uniform distributed load or a steady state thermal load. The total thickness of the plate is denoted by h with its length being a. The

length-to-thickness ratio (i.e., *a/h*) is assumed, unless otherwise mentioned, to be 15 in all numerical examples. Also the total thickness of the plate (*h*) is considered to be 0.01 m. It is assumed that the bottom surface of the plate is rich of metal (Aluminum) and the top surface is rich of ceramic (Zirconia). The thermomechanical properties of Aluminum and Zirconia are as follows [5]:

$$\begin{aligned} &E_m = 70\,\text{GPa}\,, \quad \nu_m = 0.3\,, \\ &\alpha_m = 23\times10^{-6}/^{\circ}\text{C}\,, \quad k_m = 204\,\text{W/mK} \\ &E_c = 151\,\text{GPa}\,, \quad \nu_c = 0.3\,, \\ &\alpha_c = 10\times10^{-6}/^{\circ}\text{C}\,, \quad k_c = 2.09\,\text{W/mK}\,. \end{aligned} \tag{37}$$

Fig. 1 shows the distribution of the volume fraction of the ceramic phase through the plate thickness for various values of the power-law index *n*.

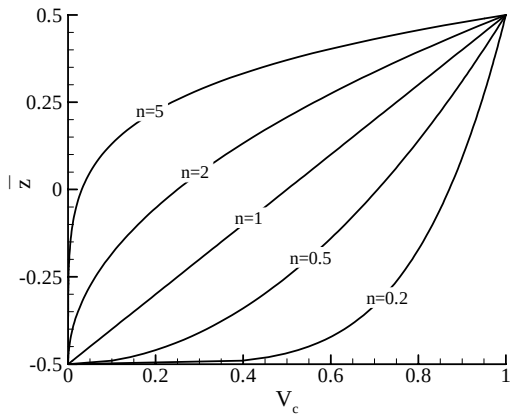

Fig. 1. Variation of the volume fraction of the ceramic phase through the thickness of the FGM plate.

In all numerical results, the linear Lagrangian interpolation function through the thickness is used. Also the total thickness of the FGM plate is divided into twenty numerical layers. In what follows, several numerical examples are presented for a plate subjected to a uniform transverse load or a steady state temperature field.

4.1 Mechanical loading

To study the nonlinear bending behavior of functionally graded plates subjected to a transverse uniform load, many examples were solved numerically. In the perturbation technique, third order, as given by Eqs. (34)-(36) were used. In the numerical results the various non-dimensional parameters used are:

$$\begin{aligned} &\text{length } \bar{x} = x/L \\ &\text{thickness } \bar{z} = z/h \\ &\text{deflection } \bar{w} = w/h \\ &\text{longitudinal stress } \bar{\sigma}_x = \sigma_x h^2/(q_0 a^2) \\ &\text{load parameter } \bar{q} = q_0 a^4/(E_m h^4)\,. \end{aligned} \tag{38}$$

Here, q_0 denotes the intensity of the applied uniform load. When the edges of the plate have S3 and C3 supports, it can be shown that the nonlinear and linear results are identical. Here, for brevity, we will only present the numerical results for C1-C1 supports.

Fig. 2 presents the variation of the center deflection of the FGM plate with *n*=2 versus the load parameter $\bar{q}$. It is seen that for the maximum deflections greater than 0.3*h* a nonlinear solution is required. Fig. 3 illustrate the variation of non-dimensional longitudinal stress $\bar{\sigma}_x$ along the top surface of this plate, when $\bar{q} = -80$. To check the correctness and accuracy of the present method, the results achieved from this theory are compared with those obtained by utilizing the commercial finite element package of ANSYS. It is to be noted that the plate has been modeled in ANSYS by using three-dimensional eight-noded structural solid elements and the total thickness of the plates has been subdivided into twelve layers. It can be seen from this figure that very good agreement is obtained using the mentioned method. Also it is observed that the exact method and perturbation technique yield identical results.

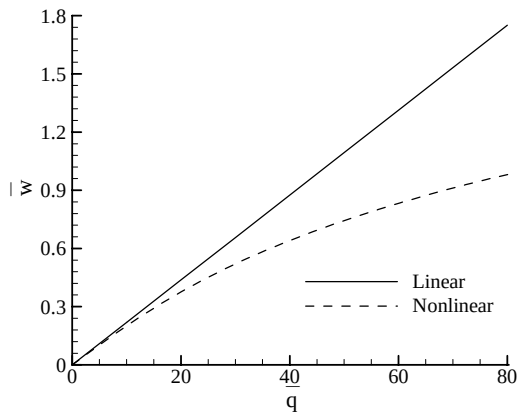

Fig. 2. Variation of non-dimensional center deflection $\bar{w}$ of the FGM plate with *n*=2 versus $\bar{q}$.

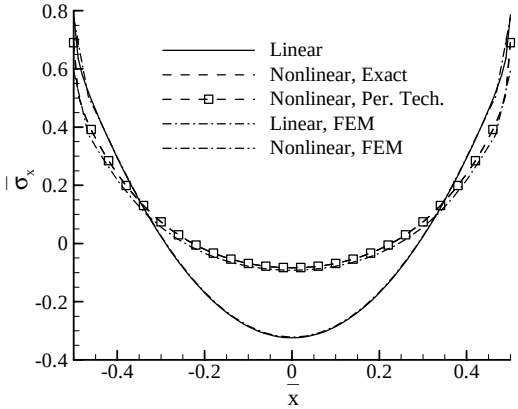

Fig. 3. Variation of non-dimensional axial stress $\bar{\sigma}_x$ along the top surface of the FGM plate with n=2 subjected to $\bar{q} = -80$.

Fig. 4 illustrates the variation of the non-dimensional center deflection of the FGM plate with different values of the power-law index n subjected to a uniform pressure. Also variation of the non-dimensional center deflection $\bar{w}$ of the FGM plate subjected to $q = -1\times10^6$ N/m^2 versus length-to-thickness ratio *a/h* for various values of the power-law index n are displayed in Fig 5. The results show that a pure metal plate has highest deflection. This is expected because the fully metal plate is the one with the lower stiffness than the ceramic and FGM plates.

Fig. 6 shows through the thickness distribution of the non-dimensional axial stress $\bar{\sigma}_x$ of the FGM plate subjected to $\bar{q} = -70$ for various values of the power-law index n. Under the application of the pressure loading, the stresses are compressive at the top surface and tensile at the bottom surface.

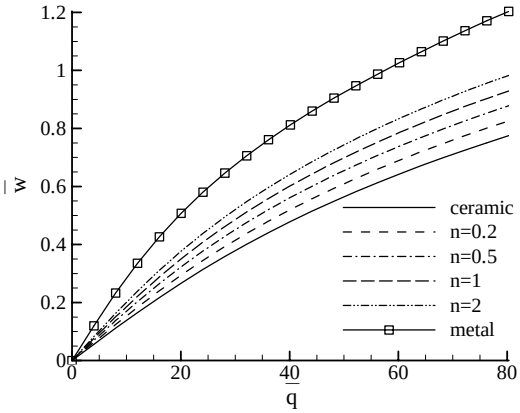

Fig. 4. Variation of the non-dimensional center deflection $\bar{w}$ of the FGM plate.

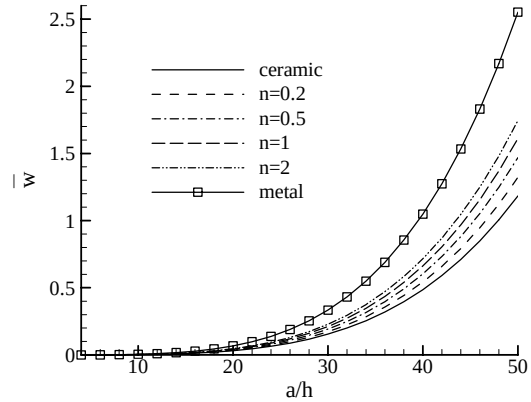

Fig. 5. Variation of non-dimensional center deflection $\bar{w}$ of the FGM plate versus length-to-thickness ratio *a/h*.

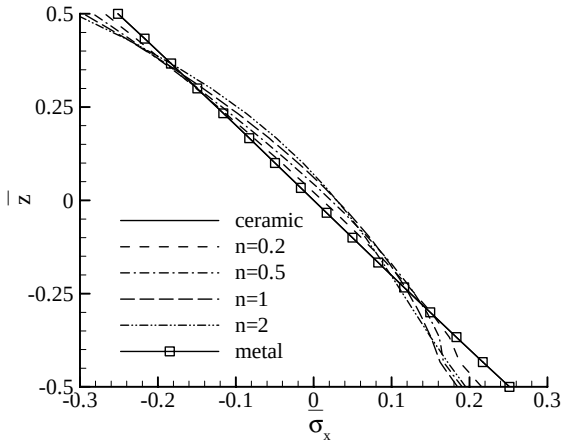

Fig. 6. Through the thickness distribution of non-dimensional axial stress $\bar{\sigma}_x$ of the FGM plate subjected to $\bar{q} = -70$.

4.1 Thermal loading

Here we present some numerical results for a representative simply supported plate (S1-S1) which is subjected to a thermal loading through its thickness direction. The temperature of the bottom metal-rich surface is kept constant at T_m=20°C and that of the top ceramic-rich surface is varied form T_c=20°C to T_c=300°C. A Stress free temperature T_0= 20°C is assumed. The temperature field through the thickness of the plate can be easily obtained from Eq. (13).

Figure 7 shows the variation of the temperature through the thickness of the FGM plate for various values of the power-law index n. It is seen that the temperature in the plates with both ceramic and

metal is always greater than that corresponding to a fully ceramic or fully metal plate.

Variation of non-dimensional deflection $\bar{w}$ along the length of the FGM plate with n=2 when T_c=200°C and T_c=300°C are shown in Fig. 8. The results of the linear analysis are also presented in the figure to highlight the difference between linear and nonlinear responses with increasing the temperature of ceramic-rich surface. From the figure it can be observed that at higher temperature nonlinear effects are predominant and deflection values are greater than the linear ones owing to the decreased structure stiffness due to contribution from the nonlinear terms in the strain field.

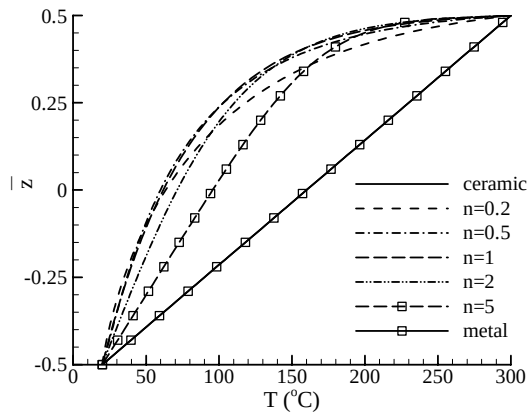

Fig. 7. Temperature profile through the thickness of the FGM plate.

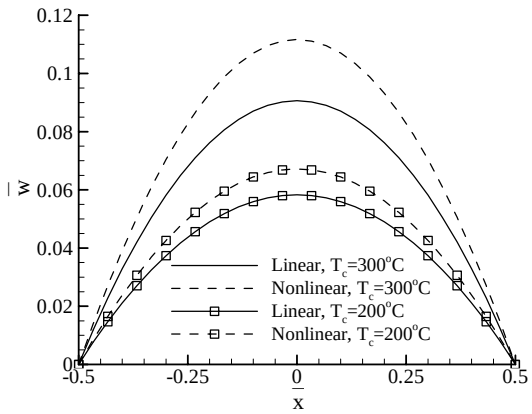

Fig. 8. Variation of non-dimensional deflection $\bar{w}$ along the length of the FGM plate with n=2.

Figs. 9 and 10 show, respectively, the linear and nonlinear variations of the non-dimensional center deflection $\bar{w}$ with increasing the temperature of the top surface for the FGM and fully metal and ceramic plates. By comparing Fig. 9 with Fig. 10, it is observed that the effect of nonlinearity increased the center deflection of the plates. Also it is seen form these figures that the fully metal plate has greater center deflection in compared to FGM and fully ceramic plates. It is to be noted that the deflection depends on the product of the temperature and the thermal expansion coefficient. Therefore, the response of the graded plates is not intermediate to the metal and ceramic plates. The deflection of the FGM plate corresponding to n = 0.2 seems to be a minimum. Note that the temperature profiles for the various plates are close to each other, and this probably is the reason why the deflections under temperature field for the various graded plates are also close to each other.

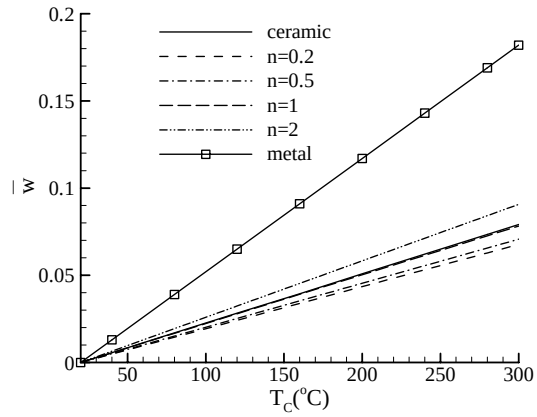

Fig. 9. Linear variation of the non-dimensional center deflection $\bar{w}$ with increasing the temperature of the top surface of the FGM plate.

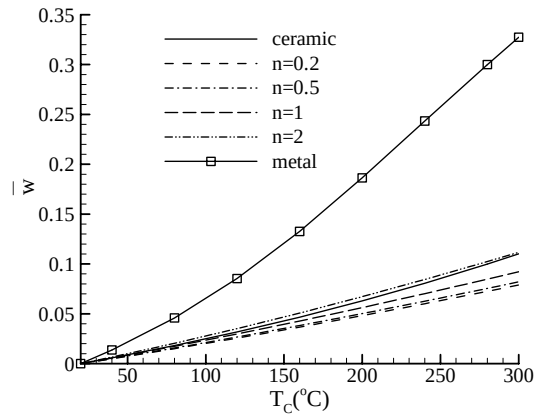

Fig. 10. Nonlinear variation of the non-dimensional center deflection $\bar{w}$ with increasing the temperature of the top surface of the FGM plate.

Finally, distribution of non-dimensional deflection $\bar{w}$ along the length of the C1-S1 FGM plate with n=2 when T_c=200°C and T_c=300°C are shown in Fig. 11. It is seen that the nonlinearity

effect is also significant in this kind of boundary condition.

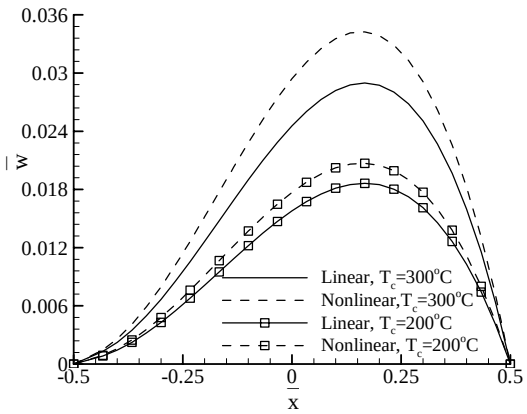

Fig. 11. Variation of non-dimensional deflection $\bar{w}$ along the length of the C1-S1 FGM plate with n=2.

5 Conclusions

In this study, based on a layerwise theory, FGM plates in cylindrical bending subjected to thermomechanical loadings are analyzed. The nonlinear strain-displacement relations are used to study the effect of geometric nonlinearity. The equilibrium equations are solved exactly and also by using a perturbation technique. The results obtained from these two methods are presented for various loading and boundary conditions. The numerical results show that the nonlinearity effect on the plate responses is significant. On the other hand, the results indicate that the effect of nonlinearity is to lower the magnitude of the transverse deflection in mechanical loading and is to higher in thermal loading. Finally, it is shown that in thermal loading case deflection in the center of fully metal plate is higher than that of fully ceramic and FGM plates.

References

[1] Noda, N. and Tsuji, T. "Steady thermal stresses in a plate of functionally gradient material". *Transactions of Japan Society of Mechanical Engineers Series A*, Vol. 57, pp. 98–103, 1991.

[2] Tanigawa, Y., Akai, T., Kawamura, R. and Oka, N. "Transient heat conduction and thermal stress problems of a nonhomogeneous plate with temperature-dependent material properties". *Journal of Thermal Stresses*, Vol. 19, pp. 77-102, 1996.

[3] Reddy, J.N. and Chin, C.D. "Thermoelastical analysis of functionally graded cylinders and plates". *Journal of Thermal Stresses*, Vol. 21, pp. 593-626, 1998.

[4] Praveen, G.N. and Reddy, J.N. "Nonlinear transient thermoelastic analysis of functionally graded ceramic-metal plates". *International Journal of Solids and Structures*, Vol. 35, No. 33, pp 4457-4476, 1998.

[5] Reddy, J.N. "Analysis of functionally graded plates". *International Journal for Numerical Methods in Engineering*, Vol. 47, pp 663-684, 2000.

[6] Reddy, J.N. and Cheng, Z.Q. "Three-dimensional thermo-mechanical deformations of functionally graded rectangular plates". *European Journal of Mechanics A/Solids*, Vol. 20, pp. 841–855, 2001.

[7] Shen, H.-S. "Nonlinear bending response of functionally graded plates subjected to transverse loads and in thermal environments". *International Journal of Mechanical Sciences*, Vol. 44, pp. 561-584, 2002.

[8] Woo, J. and Meguid, S.A. "Nonlinear analysis of functionally graded plates and shallow shells". *International Journal of Solids and Structures*, Vol. 38, pp. 7409-7421, 2001.

[9] Yang, J. and Shen, H.-S. "Non-linear analysis of functionally graded plates under transverse and in-plane loads". *International Journal of Non-Linear Mechanics*, Vol. 38, pp 467-482, 2003.

[10] Tahani, M., Torabizadeh, M.A. and Fereidoon, A. "Nonlinear analysis of functionally graded beams". *Journal of Achievements in Materials and Manufacturing Engineering*, Vol. 18, No. 1-2, pp 315-318, 2006.

[11] Hsieh, J.-J. and Lee, L.-T. "An inverse problem for a functionally graded elliptical plate with large deflection and slightly disturbed boundary". *International Journal of Solids and Structures*, Vol. 43, No. 20, pp. 5981-5993, 2005.

[12] Agarwal, S., Chakraborty, A. and Gopalakrishnan, S. "Large deformation analysis for anisotropic and inhomogeneous beams using exact linear static solutions". *Composite Structures*, Vol. 72, pp. 91–104, 2006.

[13] Fung, Y.C. "*Foundation of solid mechanics*". Englewood Cliffs, New Jersey: Prentice-Hall, 1965.

[14] Tahani, M. and Nosier, A. "Accurate determination of interlaminar stresses in general cross-ply laminates". *Mechanics of Advanced Materials and Structures*, Vol. 11, No. 1, pp. 67-92, 2004.

[15] Franklin, J.N. "*Matrix theory*". Englewood Cliffs, New Jersey: Prentice-Hall, 1968.

Appendix

The coefficient matrix $[A]$ and vector $\{F\}$ appearing in Eqs. (24) are defined as:

$$[A]=\begin{bmatrix} [0] & [I] & \{0\} & \{0\} \\ [a_1] & [0] & \{0\} & [a_2] \\ \{0\}^T & \{0\}^T & 0 & 1 \\ \{0\}^T & \{b_1\}^T & b_2 & 0 \end{bmatrix}, \quad \{F\}=\begin{Bmatrix} \{0\} \\ \{0\} \\ 0 \\ f \end{Bmatrix}$$

where [0] and [I] are $(2N+4)\times(2N+4)$ square and zero identity matrices, respectively, and $\{0\}$ is a zero vector with $2N$+4 rows. The remaining matrices in the above equations are:

$$[a_1]=([D_{11}]-\{B_{11}\}\{B_{11}\}^T/A_{11})^{-1}([A_{55}]+[\varepsilon])$$
$$[a_2]=([D_{11}]-\{B_{11}\}\{B_{11}\}^T/A_{11})^{-1}\{A_{55}\}$$
$$\{b_1\}=-\{A_{55}\}/(A_{55}+N_x^0)$$
$$b_2=\varepsilon/(A_{55}+N_x^0)$$
$$f=-q_0/(A_{55}+N_x^0)\,.$$